Journal of Fluids and Structures (2002) **16**(5), 581–595
doi:10.1006/jfls.444 available online at http://www.idealibrary.com on IDEAL®

EXPERIMENTAL 3-D SIMULATION OF THE COMPRESSION WAVE, DUE TO TRAIN–TUNNEL ENTRY

M. Bellenoue, V. Morinière and T. Kageyama

Laboratoire de Combustion et de Détonique (UPR 9028 CNRS)
F-86961 Futuroscope, France

(Received 28 April 1999; and in final form 23 October 2001)

The work presented in this paper concerns the first compression wave generated in a tunnel when a high-speed train enters it. This wave is the first of successive compression and expansion waves which propagate back and forth in the tunnel. Once generated at the tunnel entrance, its amplitude and gradient vary according to the train and tunnel characteristics. These waves provoke: (a) an aural discomfort for train passengers, (b) mechanical stresses on train and tunnel structures, and (c) emission of impulsive noises outside the tunnel. A reduced-scale test method, using low-sound-speed gas mixtures, has been developed and validated by using newly available European full-scale test-results. It can reproduce quite well the three-dimensional effects due to the train geometry and its position in the tunnel. The study also clearly points out that three-dimensional effects on the front of the first compression wave are attenuated with distance from the tunnel entrance and that the wave front can be considered well established and planar for distances larger than four times the tunnel diameter. Characteristics of the planar wave are in good agreement with Japanese results. The reduced-scale train Mach number has been extended up to 0.34 to determine its test domain. Our study clearly shows that, as far as the characteristics of the wave front of well-established planar first compression wave are concerned, axially symmetrical models can advantageously replace three-dimensional models, provided that the longitudinal cross-sectional area profile is the same for both configurations. This feature yields the following train nose design procedure: first determine the cross-sectional profile of a train nose against train–tunnel interactions by means of axially symmetrical configuration, then give a three-dimensional shape for drag and stability optimisation.

1. INTRODUCTION

When a train enters a tunnel, it replaces the air inside the tunnel, producing different phenomena. Part of it runs backwards around the train body and exits from the tunnel entrance as a jet (Auvity *et al*. 2001). This phenomenon stops when the train tail finishes entering the tunnel (Kage *et al*. 1992). The remaining part of the air in the tunnel is pushed by the train nose and flows in front of it. It generates a compression wave, propagating in the tunnel at the local sound velocity which is faster than the train speed. This compression wave is reflected at the tunnel end as an expansion wave that goes back towards the train, and finally to the tunnel entrance. In turn, this expansion wave is reflected as a compression wave at the tunnel entrance. These repeated propagations and reflections inside the tunnel progressively attenuate the pressure waves. Moreover, every time a compression wave is reflected at the end of the tunnel, part of its energy is emitted outside

0889-9746/02/050581 + 15 $35.00/0

from the tunnel exit as an impulsive pressure wave called a micro-pressure wave. Its amplitude is proportional to the pressure gradient of the oncoming compression wave (Ozawa 1979; Ozawa *et al*. 1993). For a strong compression wave, it becomes so important that the people living near tunnel exits suffer from noise, and housing structures have to withstand vibrations similar to those caused by aeronautical "sonic booms". This problem, well known in Japan (Ozawa 1979; Maeda *et al*. 1993), can occur in Europe due to the development of high-speed train networks. The compression and expansion waves that propagate back and forth in the tunnel also create direct adverse effects, such as aural discomfort for passengers during tunnel passing, and generation of rapid changing forces on the train itself and on the tunnel internal structures. The amplitude and the gradient of the compression waves can be attenuated in different manners. The most effective one is the reduction of the train speed, but for a high-speed train operation this is used only in critical conditions, such as the crossing of two trains in a tunnel. The others consist of optimising the geometry of the train nose and the tunnel entrance. However, the train nose geometry cannot be determined only to solve the problems described above. Indeed, in general, in railway operations, a train nose becomes a train tail on its return trip and its geometry is a decisive factor for the train stabilisation (Kohama *et al*. 1994). Thus, the train nose geometry must take these two conditions into account.

Although such transient aerodynamic phenomena have been studied for a long time (Fox & Vardy 1973; Ozawa 1979; Woods & Pope 1979), they have become more pertinent for the discomfort of passengers, for the lifetime of rolling stocks and for their reliable operation, because of the continuous velocity increase of high-speed trains. These studies have been performed either numerically or experimentally. Thanks to the progress of computational fluid dynamics, very detailed investigations are now possible by numerical means (Iida 1994; Ogawa & Fujii 1996; Grégoire *et al*. 1997), but full-scale investigations are always necessary to point out new problems and to validate numerical results. Well-documented experimental simulations using reduced-scale models are attractive alternatives to full-scale tests, because of their cost saving and the possibility that they offer to separate different parameters. In certain conditions, calculations in numerical simulations become too time-consuming because of the fine mesh required to describe the train and the tunnel, and reduced-scale tests become preferable. Reduced-scale tests must also be validated by full-scale test results. It is one of the reasons why a European Union research project TRANSAERO (Transient Aerodynamics for Railway system Optimisation) has been carried out in the framework of Brite EuRam III of European Union (Matschke 1999). The validation of the method presented in this paper stands on newly available full-scale test data obtained in this context.

The work presented here focuses on the first compression wave generated in the tunnel by a high-speed train. Indeed, it is the very wave that is the most powerful factor, and its control is the key to all solutions. The most important parameters affecting the above-mentioned pressure wave are the train Mach number M, the train/tunnel blockage ratio $S_{\mathrm{Train}}/S_{\mathrm{Tunnel}}$ (train nominal cross-sectional area divided by the tunnel nominal cross-sectional area), the train nose geometry and the tunnel entrance geometry. It has been proved that the maximum value of the compression wave amplitude increases with the train speed squared, and that of its temporal derivative and the micro-pressure wave amplitude vary approximately with the train speed cubed (Swarden 1973; Ozawa 1979; Woods & Pope 1981; Kage *et al*. 1992; Iida 1994; Auvity & Kageyama 1996; Howe 1998*a*). Moreover, when the initial pressure gradient of the compression wave is high enough, it can increase along the tunnel (Ozawa 1979; Aoki *et al*. 1995) because of the compressibility of the air and the adverse effects become more severe. One of the efficient ways to attenuate them is to increase the initial wave thickness. Several solutions such as

lengthening the train nose (Maeda *et al.* 1993; Bellenoue *et al.* 1999; Iida *et al.* 1996) or the use of enlarged or flared tunnel entrances with or without perforation (Ozawa & Maeda 1988; Ozawa *et al.* 1991; Howe 1998*b*; 1999) have been tested and their effectiveness has been proved.

The objectives of this paper are to present: (i) the validation, in a three-dimensional configuration (Matschke 1999), of a reduced-scale test method dedicated to study the generation of the first compression wave; (ii) the degree of agreement with full-scale tests that our results give in different configurations (Matsuo *et al.* 1997); (iii) the justification of the use of axially symmetric train models in place of true three-dimensional ones, in the case where interest is limited to the well-established planar compression wave.

2. EXPERIMENTAL SET-UP

Several well-known experimental devices, such as the test rig of British Rail Research, or the one of the Railway Technical Research Institute in Japan, have been exploited for a long time. In both installations, reduced models are rather large (reduction ratio higher than 1/30) and a finite length train passes through a finite length tunnel. The former is well adapted to 3-D configurations, and the maximum speed of its model trains is limited to 280 km/h, even after recent improvements to the test rig (Johnson 1999). The RTRI model can reach a speed of 360 km/h, but according to published results, tests are generally performed in axially symmetric configurations. The test-rig of the University of Tohoku (Sasoh *et al.* 1994) is very small (reduction ratio of 1/300). The reduction ratios of the test rigs of NLR, Nationaal Lucht-en Ruimtevaartlaboratorium [reduction ratio of 1/175; Demmenie *et al.* (1998)] and ENSMA, Ecole Nationale Supérieure de Mécanique et d'Aérotechnique [reduction ratio of 1/140; Auvity & Kageyama (1996)] allow studies of the established planar compression wave. However, train diameters, of order of 20 mm, are too small to realise detailed 3-D models. The NLR experimental set-up can perform tests either in axially or non-axially symmetric configurations. With this set-up, the train speed is able to reach about 600 km/h. Accurate positioning of the train in the tunnel is, however, difficult for high-speed tests, because the train model is not connected to its two guide-rails. The set-up used by Auvity (1998) can perform tests in axially symmetric configurations and its speed is limited to 180 km/h.

The installation used for this study is dedicated to the study of the first compression wave generated by the entry of a train in a tunnel. It is based on the use of low-sound-speed gaseous mixtures in place of air (Swarden 1973). To reach high Mach numbers with limited train speed, mixtures composed mainly of SF_6 and air have been used, which can reduce the sound speed down to 135 m/s. Train Mach numbers up to 0·40 can then be realised with a train speed of 55 m/s. The limitation of the train speed is due to the capacity of the propulsion system. The validity of this method to predict phenomena occurring in atmosphere was first confirmed by our previous work (Grégoire *et al.* 1997). In this device, an axially symmetric train (2-D) or a fully 3-D train enters a tunnel with a constant speed and stops after having travelled a sufficient distance to correctly generate the first compression wave. The experimental device (Figure 1) consists of an air gun, a moving piston pushing a circular cylindrical train support (50 mm in diameter), and a tunnel placed in a tank containing gaseous mixtures. An area of 0·3 m^2 on the upper wall of this tank is open to the atmosphere just above the train. For both 3-D and axially symmetric tests, a model representing the first vehicle of a train is attached at the end of the support. The geometric reduction ratio of the test rig is 1/77.

The principle of a test is as follows: when the membrane of the air gun is broken, air in the high-pressure chamber is discharged behind the piston; the speed of the model train

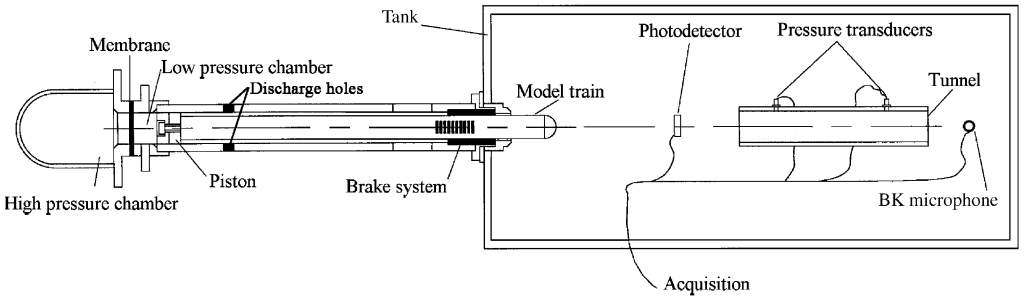

Fig. 1. Experimental apparatus.

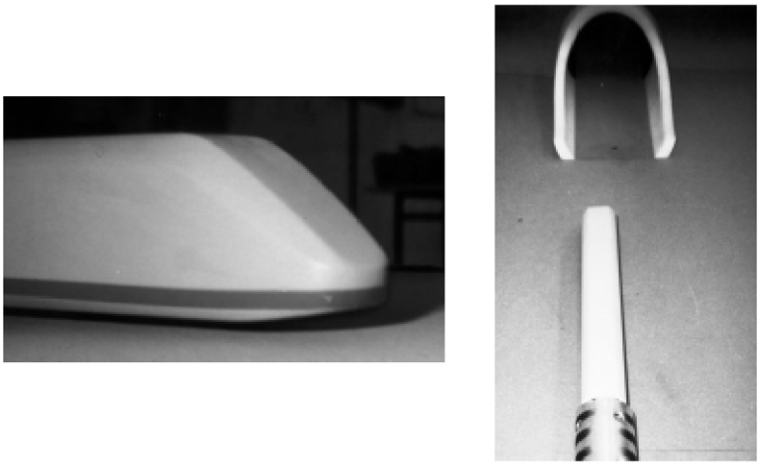

Fig. 2. ETR 500 nose and the north portal.

increases until the piston reaches the discharge holes. Then the compressed air behind the piston exits into the atmosphere and the model train maintains a constant speed thanks to its inertia. Finally, the brake system stops the train. In our experiment, the train reaches a constant speed 350 mm before it enters the tunnel, and it maintains this constant speed for a distance of 390 mm inside it. The distance thus realised is enough to correctly generate the first compression wave. Here, 390 mm at our reduced scale corresponds to about 30 m at full scale. Before a test, the train model is positioned at the entrance of the tank in order to minimise all effects due to the start of the train.

To validate our reduced-scale test method against full-scale tests, experiments have been realised by means of a tunnel model which reproduces the first 265 m from the north entrance of the Terranuova le Ville tunnel on the Diretissima line of the F.S. in Italy (Figure 2). The nominal cross-sectional area of this tunnel (69 m^2) is relatively small. Its equivalent diameter d_T is therefore equal to 9·4 m. The concrete tunnel wall is represented at reduced scale by the inner surface of a stainless-steel tube, the half ballast track by a polyethylene foam plate. The half-open entrance hood is machined from a synthetic resin block. According to Howe (1999), to obtain the right compression wave, the topology outside the tunnel mouth has to be reproduced completely. In our model, a retracted vertical wall of polyethylene foam is used to replace the sod coverage on the tunnel mouth. The unsteady flow exiting from the tunnel entrance during the train entry creates a vortex

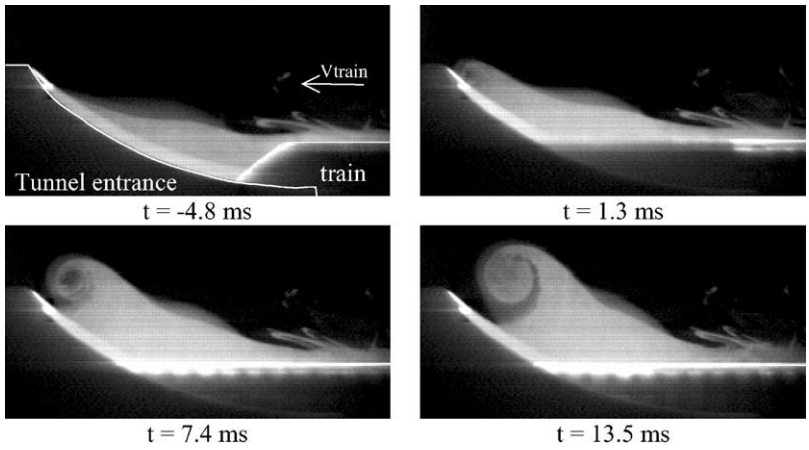

Fig. 3. Laser sheet visualisation of exiting flow, $V_{\text{train}} = 40\,\text{m/s}$. ($t = 0$ is the time when the train nose tip reaches the constant section of the tunnel $x = 0$).

(Auvity *et al*. 2001). Figure 3 shows that this vortex is displaced along the train body from the exit and does not interact with the environment behind the entrance hood. So, the reproduction of the nearby hills is not necessary because they are sufficiently far. The tunnel length has been adjusted to 3·5 m, so that the expansion wave generated by the reflection of the compression wave at the tunnel exit does not disturb the measurement of the fully developed planar compression wave at the points farthest from the entrance. Details of the train models will be described later, with the test conditions.

The parietal pressure relative to the atmospheric pressure is measured at seven stations along the tunnel wall, corresponding to those used during full-scale tests (Matschke 1999): $X_1 = 8\,\text{m}$, $X_2 = 23\,\text{m}$, $X_3 = 43\,\text{m}$, $X_4 = 80\,\text{m}$ and 2·5 m in height on the left-hand side and $X_5 = 23\,\text{m}$, $X_6 = 43\,\text{m}$, $X_7 = 80\,\text{m}$ and 2 m in height on the right-hand side ($X = 0$ corresponds to the beginning of the constant section of the tunnel).

The train speed V_{Train} was determined by means of a home-made device using an opto-electronic transducer (Honeywell model HOA1180-003). An example of a curve representing the train speed in function of time is presented in Figure 4. The velocity fluctuation of about 2% observed between $t = -0{\cdot}005\,\text{s}$ and $0{\cdot}015\,\text{s}$ is due to the limits of time scale discretisation. The train speed is constant during the train entry into the tunnel and the uncertainty on the train mean velocity can thus be considered to be less than 1%. Pressures, relative to the atmospheric pressure, were measured by means of rapid-response pressure transducers (ENDEVCO model 8510B-2) which were flush-mounted on the tunnel wall. Data acquisition was realised by means of a 12 bits-resolved, variable scale, numerical data acquisition system. The cumulative uncertainty of the pressure measurement is less than 50 Pa. All data are sampled at a rate of 33 kHz. Due to the noise in the excitation current of the transducers, pressure evolutions are filtered before determining the evolutions of the pressure gradient.

For each run, the sound speed of the mixture was directly measured in the tank by means of the time necessary for an acoustic pulse to propagate between two positions. Given the sound speed and characteristics of the constituent gases (cf. Table 1), the mixture density ρ and its specific heat ratio $\gamma(= c_p/c_v)$ have been determined by thermodynamic relations. Then, train speed, pressure and pressure gradient have been converted to corresponding non-dimensional parameters such as Mach

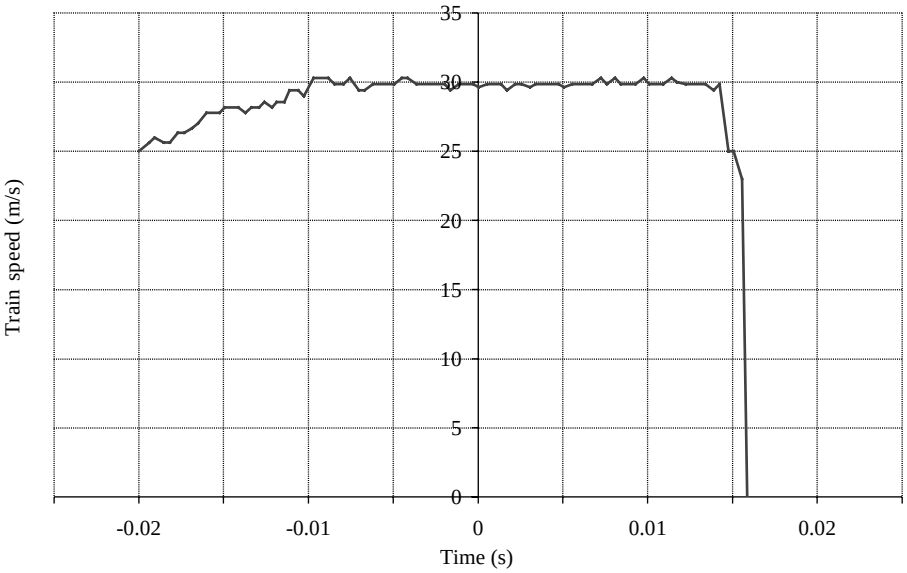

Fig. 4. Train speed versus time ($t = 0$ corresponds to the time when the tip of the train nose reaches the beginning of the constant section of the tunnel $X = 0$).

TABLE 1

Gas characteristics for air and SF_6 at 298 K and 1 atm

	Molecular weight ($g\,mol^{-1}$)	Heat capacity ($kJ\,kg^{-1}\,K^{-1}$)	Density ($kg\,m^{-3}$)	Viscosity $\times 10^7$ ($N\,s\,m^{-2}$)
Air	29	1·01	1·19	184·6
SF_6	146·05	0·665	5·97	150

number M, pressure coefficient $C_p = \Delta p/[\frac{1}{2}\gamma p M^2]$, and pressure gradient coefficient $K_{gr} = [\mathrm{d}(\Delta p)/\mathrm{d}t]/[\frac{1}{2}\gamma p c M^3/d_t]$, where Δp is the over local pressure compared to the atmospheric pressure p and c the local sound speed.

In our previous study (Grégoire *et al*. 1997), a comparison between results obtained at reduced scale in air and that obtained in low-sound speed mixtures for the same train Mach numbers has proved the possibility of the transposition of data obtained in these two different environments. So, results obtained by our reduced-scale tests have been converted to the physical values of the full-scale configuration, to facilitate the comparison between the results obtained during reduced-scale and full-scale tests.

3. RESULTS AND DISCUSSION

3.1. Simulation of Three Dimensional Phenomena

The ability of reduced-scale tests to reproduce 3-D phenomena observed during full-scale tests was examined for a configuration in which an ETR 500/92 train passes through the Terranuova le Ville Tunnel (Matschke 1999). The ETR 500/92 has a short nose (about 4 m long) and a large cross-sectional area (about 10·6 m^2). The resulting train/tunnel blockage ratio S_{Train}/S_{Tunnel} is 0·15. For this study, a 1/77 scale 3-D model of the first

vehicle was attached to the cylindrical train support (Figure 2). The length of the train model is 350 mm. The train runs on the left-hand side, thus the free area on the left side in the tunnel is smaller than that of the opposite side.

Figure 5 shows the successive steps of the establishment of the first compression wave in a full-scale test and in a corresponding reduced-scale test. The train Mach number is equal to 0·2. The time $t = 0$ corresponds to the instant when the train nose tip enters into the nominal section of the tunnel. Figure 5(a) shows measurements at the beginning of the tunnel, at $X_1 = 8$ m. For this point, pressure has been measured only on the left side. From Figure 5(b) to Figure 5(d), the distance of the measuring points from the tunnel entrance increases (Figure 5(b): $X_2 = X_5 = 23$ m, Figure 5(c): $X_3 = X_6 = 43$ m, $X_4 = X_7 = 80$ m). For these points, pressures have been measured on both sides.

We first examine the overall reproduction quality. On all four figures, we can observe that the pressure histories measured in the reduced-scale test follow quite well each phase of the establishment of the first compression wave measured in the full-scale test. Especially, it is worth noting that the reduced-scale tests can clearly reproduce the difference between pressure signatures on the left- and right-hand sides of the tunnel, which is due to the available free air passage between the train and the tunnel wall and is typically a three-dimensional effect. In Figs. 5(b) and 5(c), an arrow indicates an overpressure on each curve of the narrower (left) side pressure signals. Such an overpressure is absent on the larger (right) side signals. These overpressures occur at the passage of the nose shoulder by the pressure transducers.

After the passage of the nose shoulder by the pressure gauge, the pressure returns to the atmospheric value. For $X_3 = X_6 = 43$ m, Figure 5(c), the pressure decreasing phase, corresponding to the passage of the nose shoulder by the pressure transducer, occurs later than that observed during full-scale tests. This means that the model train begins to decelerate between $X_2 = X_5 = 23$ m and $X_3 = X_6 = 43$ m. Nevertheless, the compression wave is completely generated at the position $X = 43$ m. Moreover, the examination of the phase diagrams, obtained in our earlier tests under similar conditions (Grégoire *et al.* 1997), confirms that the compression wave propagates upstream of the train without being perturbed by the expansion wave generated by the train deceleration.

We now examine the results quantitatively. The maximum pressure difference between full-scale and reduced-scale results is limited to 6%, except at the position $X_6 = 43$ m [cf. Figure 5(c)], where the pressure difference rises up to around 9%. Comparisons of results obtained for a train Mach number equal to 0·225 have also given the same tendencies in terms of discrepancies. Note that the pressure measurements at the right side in the full-scale test ($X_6 = 43$ m and $X_7 = 80$ m) give lower values (6%) than at the left side (X_3 and X_4). As the pressure wave must be plane at $X = 43$ and 80 m, the reason for this discrepancy is not well identified (niches effects?...). However, the results at $X = 187$ m in full-scale test give the same evolution on the both sides.

As the main problems due to the pressure waves occur during the reflection of the first compression wave at the end of the tunnel (sonic boom) and the propagation of the resulting expansion wave (stress on the train body or on the tunnel), knowing the characteristics of the planar compression wave is important. Our reduced-scale results show that as far as the interest is limited only to the well-established planar first compression wave, it is sufficient to measure the pressure at a distance from the tunnel entrance longer than four times the tunnel diameter, i.e., 43 m in the present case.

Figures 6 and 7 show the comparison of pressure gradient histories between reduced-scale tests and full-scale tests at $X = 80$ m, where the planar compression wave is well established [Figure 5(d)]. Figure 6 corresponds to a train Mach number of 0·201, while Figure 7 to a train Mach number of 0·225. In both figures, the pressure gradient histories

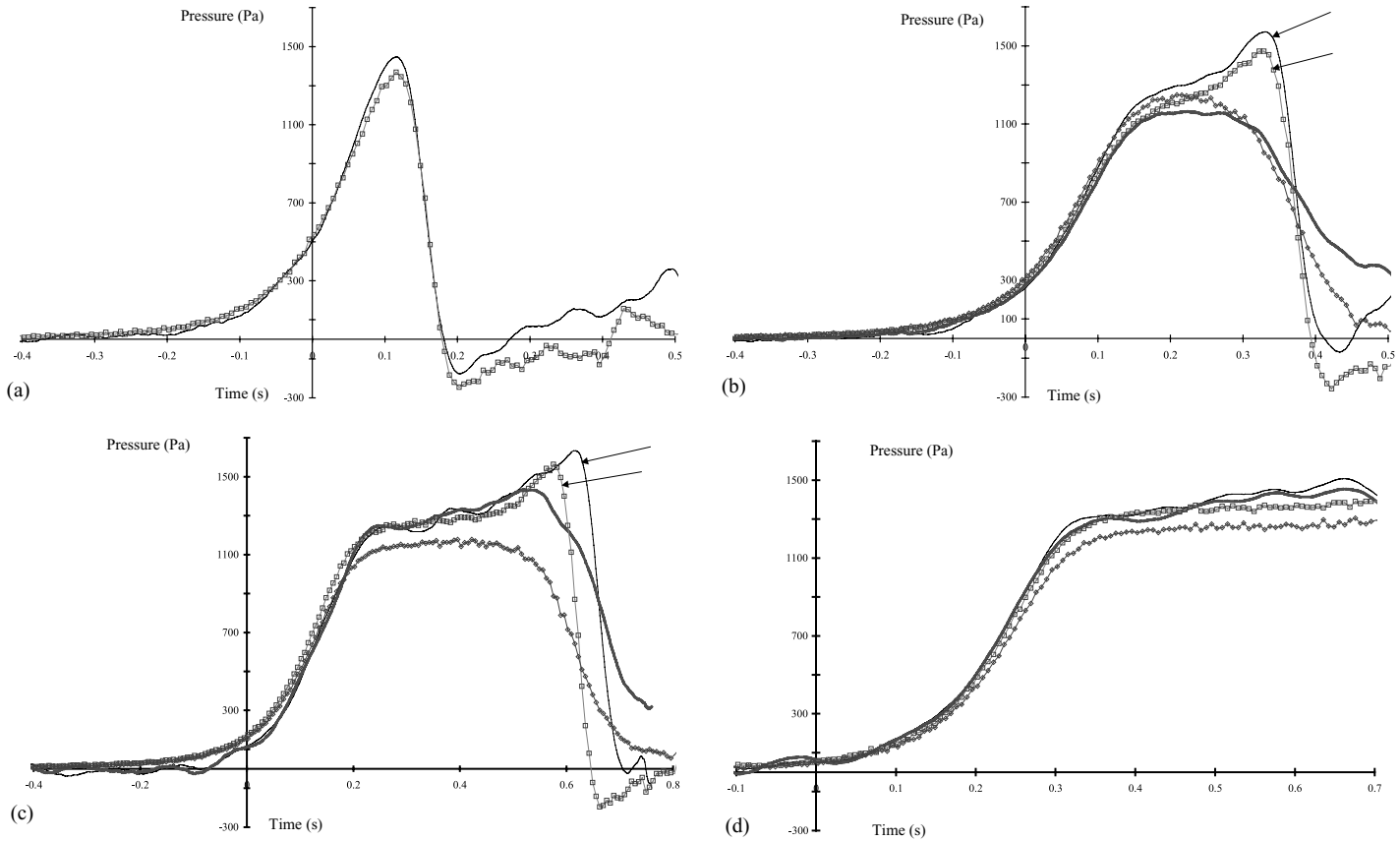

Fig. 5. Comparison between full-scale and reduced-scale tests for $M = 0.201$: (a) $X_1 = 8$ m; (b) $X_2 = X_5 = 23$ m; (c) $X_3 = X_6 = 43$ m; (d) $X_4 = X_7 = 80$ m. (–□–), full scale, left side X_1, X_2, X_3, X_4; (–◇–), full scale, right side X_5, X_6, X_7; —, reduced scale, left side X_1, X_2, X_3, X_4; (▬), reduced scale, right side X_5, X_6, X_7.

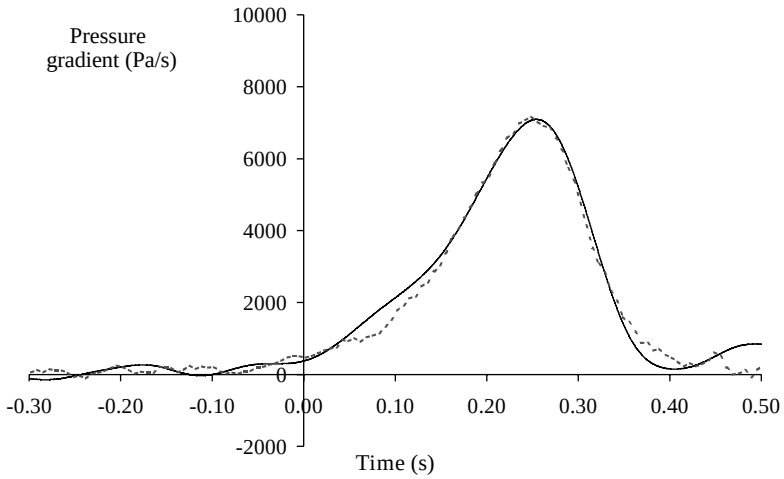

Fig. 6. comparison of the pressure gradient between full-scale and reduced-scale tests $M = 0.201$, $X = 80$ m: ——, reduced-scale test: - - -, full-scale test.

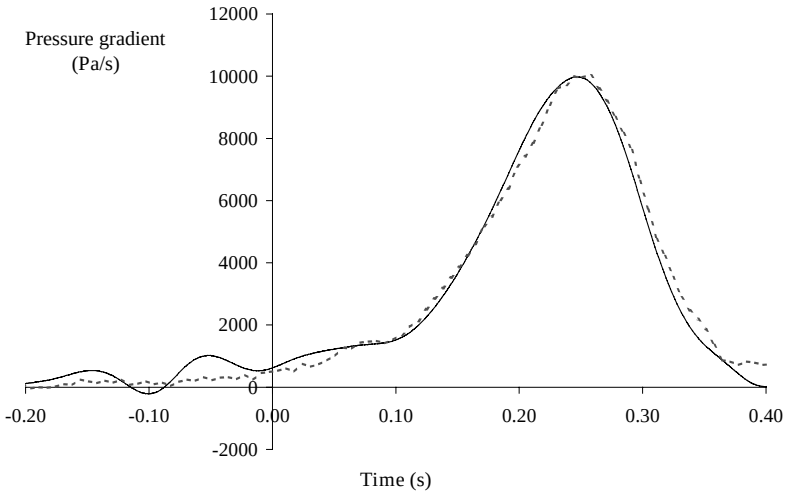

Fig. 7. Comparison of the pressure gradient between full-scale and reduced-scale tests $M = 0{\cdot}225$, $X = 80$ m: ——, reduced-scale test; - - -, full-scale test.

of reduced-scale tests follow those of the full-scale tests well. For $M = 0{\cdot}201$, the maximum value of the gradient is about 7 500 Pa/s, while it reaches 10 150 Pa/s for $M = 0{\cdot}225$. The maximum values of the gradient measured in reduced-scale tests are in general 3–5% larger than those measured in full-scale tests. Therefore, the agreement between full- and reduced-scale results can be considered satisfactory.

The results obtained show that in spite of the difference of 2 orders of magnitude in Reynolds numbers of flows around the train and behind the compression wave (respectively 60×10^4 and 8×10^4 for reduced-scale tests, and 19×10^6 and $2{\cdot}3 \times 10^6$ for full-scale tests), the compression waves generated in the reduced-scale and full-scale tunnels are the same when they become planar. As mentioned by Howe (1998*c*), this fact

means that viscous effects are negligible for the compression wave generation. We can conclude that there is no Reynolds number effect and reduced-scale tests with a scale radio of around 80 are able to reproduce phenomena occurring at full scale.

The results presented here show that the reduced-scale test rig and the method developed in this study allow the prediction of three-dimensional phenomena that occur in a real tunnel during the compression wave generation phase.

3.2. Comparison with General Formulae Deduced from Japanese Full-Scale Tests

The study has been extended to compare results obtained by our reduced-scale tests with full-scale tests performed in Japan. We focus on the sensitivity to the train Mach number of the amplitude Δp and of the maximum pressure gradient $(\mathrm{d}\Delta p/\mathrm{d}t)_{\max}$ of the compression wave. The pressure amplitude is defined by the pressure at the end of the rapid increase phase mentioned above (cf. Section 3.1). Thus, it excludes the slow pressure increase due to viscous effects between train and tunnel walls. Japanese results are represented by two best-fit formulae proposed by Matsuo *et al.* (1997):

$$\Delta p = \frac{1}{2}\gamma p M^2 \left[\frac{1-\phi^2}{\phi^2 + (1-\phi^2)M - \gamma M^2(1-\phi^2/2)}\right], \tag{1}$$

where

$$\phi = 1 - S_{\mathrm{Train}}/S_{\mathrm{Tunnel}}.$$

$$\left(\frac{\mathrm{d}\Delta p}{\mathrm{d}t}\right)_{\max} = \frac{V_{\mathrm{train}}}{\pi k d_T}\Delta p, \tag{2}$$

Here again, data corresponding to $X = 80\,\mathrm{m}$ in full-scale tests have been used to represent reduced-scale test results. Figure 8 shows the variation of the pressure amplitude and its gradient in function of the train speed V_{train} for $35\,\mathrm{m/s} \leqslant V_{\mathrm{train}} \leqslant 110\,\mathrm{m/s}$. The speed range $35\,\mathrm{m/s} < V_{\mathrm{train}} < 80\,\mathrm{m/s}$ corresponds to the full-scale tests. The pressure amplitude Δp increases from about 380 Pa for $V_{\mathrm{train}} = 40\,\mathrm{m/s}$ to 1 700 Pa for $V_{\mathrm{train}} = 80\,\mathrm{m/s}$. For the same train speed range, the maximum value of the pressure gradient increases from 1 370 to 12 000 Pa/s. Reduced-scale tests have also been performed for train speeds of about 110 m/s (about 400 km/h). Full-scale test results, with the same type of train, are not yet available for this speed range. For such a speed, the pressure amplitude reaches 3 000 Pa and the maximum value of the pressure gradient 29 000 Pa/s. Our results of the pressure amplitude agree quite well with Matsuo's equation (1) curve. For this parameter, there are different formulas deduced from different experimental results (Ozawa 1988; Grégoire *et al.* 1997). All formulas give the same tendency and give good agreement with our results.

For the maximum pressure gradient, our results fit Matsuo's curve [equation (2)] well, provided that the constant k is modified to 0·37 from the original value of 0·33. This constant partially includes the nose-geometry effect. It is now well known that lengthening the train nose decreases the amplitude of the pressure gradient (Maeda 1993). Matsuo has chosen the value of 0·33 for a train nose length of 6·75 m. As the nose length of the ETR 500 train used here is of 4 m and shorter than the Japanese one, the value of k, for our configuration, must be larger than 0·33. The dependence of this constant upon train geometry needs further investigation to also take the tunnel entrance geometry into account.

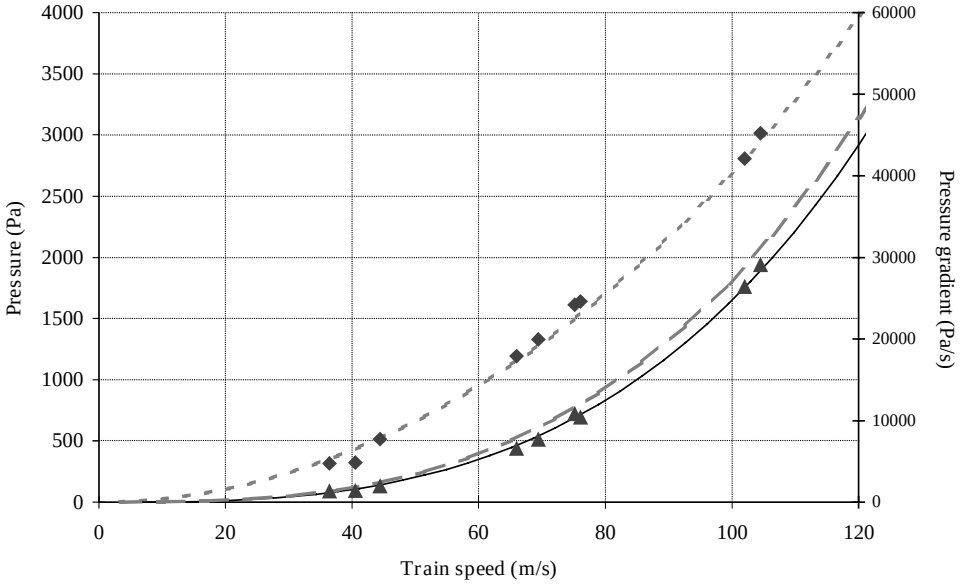

Fig. 8. Pressure and pressure gradient maximum versus train speed: ◆, pressure maximum (Pa); – – – –, pressure maximum (Matsuo *et al.* 1997); ▲, pressure gradient max (Pa/s);——, pressure gradient max (Matsuo *et al.* 1997, $k = 0{\cdot}33$); – –, pressure gradient max (Matsuo *et al.* 1997, $k = 0{\cdot}37$)

3.3. Replacement of A Three Dimensional Train Model by an Equivalent Two-Dimensional Model

As can easily be imagined, 3-D models are time and money consuming and not well adapted to systematic studies of the influence of the train shape on amplitude and gradient of the compression wave generated in a tunnel. A feasibility study of the replacement of a 3-D model by a 2-D (axially symmetric) model has therefore been undertaken. Investigation has been carried out by means of an axially symmetric model equivalent to an ETR 500 train. It has the same longitudinal profile as its corresponding 3-D model (Figure 9), the cross-sections are the same along the train length. As the details of the 2-D model are not the same as the 3-D one, the characteristics of the compression wave of both models cannot be the same during its generation. However, the comfort of passengers or the stress on train structures is largely determined by the characteristics of the expansion wave resulting from the reflection of the well-established compression wave. So, if an equivalent 2-D model can correctly reproduce the latter wave, such reduced-scale experimental simulations become more attractive.

As only the planar wave has to be considered, data obtained at $X_4 = X_7 = 80$ m have been used for this study. Note that the train always runs on the left side of the tunnel. Figure 10 shows the pressure [Figure 10(a)] and pressure gradient [Figure 10(b)] histories for a train Mach number of 0·20. Results obtained with the axially symmetric model reproduce well those obtained by the true 3-D model. Indeed, the pressure amplitude of 1 380 Pa ($t = 0{\cdot}375$ s) obtained with the 2-D model represents only a difference of 4% against that obtained with the 3-D model. This result was expected, as the amplitude of the planar compression wave can be very well estimated by a one-dimensional model (Auvity 1998). Concerning the pressure gradient, the difference of 9% is a little bit higher than that of the pressure histories but still remains reasonable. Nevertheless, this must not be

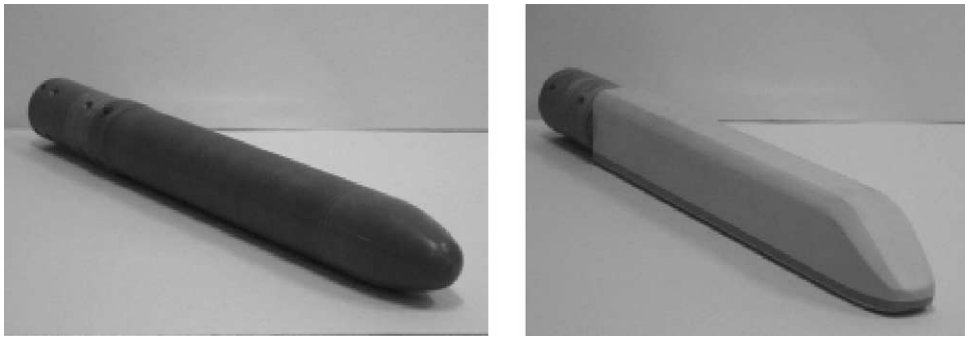

Fig. 9. Axially symmetric and 3-D noses of the ETR500 train.

considered to be only due to the 3-D effects. Indeed, as the pressure gradient is proportional to the train speed to the cube, a relative error of 1% on the train speed (cf. Section 2) induces an uncertainty of 3% on the pressure gradient amplitude. As this comparison is done on the results obtained with two independent configurations, the overall uncertainty on this pressure gradient difference can reach 6%. Therefore, if the 3-D effects during the generation of the compression wave still remain at this measuring point, its influence can be estimated to be about 5%.

From these results, we can conclude that if the interest is limited to the characteristics of the planar wave, which is often the case, it is possible to replace a true 3-D train model by an equivalent axially symmetric model. This yields the following train nose design procedure: first optimise the cross-section profile of a train nose against train–tunnel interactions by means of axially symmetrical models, then, study the three-dimensional shape for drag and stability optimisation by retaining the same area space evolution obtained previously.

4. CONCLUSION

The work presented in this paper shows the possibilities offered by a reduced-scale test method to simulate experimentally the first compression wave generated in a tunnel when a high-speed train enters it. Its validation has been realised by means of well-documented recent data, obtained during the full-scale tests carried out in the framework of the European Union research project TRANSAERO. Thanks to the use of low-sound-speed gas mixtures, the developed test device allows the simulation of the three-dimensional effects of the characteristics of the first compression wave for a train Mach number up to $M = 0{\cdot}35$. The discrepancies obtained between reduced-scale and full-scale test are less than 7% for the pressure amplitude and less than 10% for the maximum pressure gradient. Moreover, we show that three-dimensional effects are attenuated with the distance from the tunnel entrance and that the planar wave is clearly established after the generated compression wave has propagated four times the tunnel diameter inside the tunnel ($X = 43$ m). Tests have been extended for speeds of about 400 km/h to predict the values of the two above-mentioned parameters not yet measured in full-scale tests with corresponding materials.

Comparisons, by means of a formula proposed by Matsuo *et al.*, show that our results for the pressure amplitude are in good agreement with those obtained on the Japanese Shinkansen. For the maximum value of the pressure gradient, it is pointed out that the

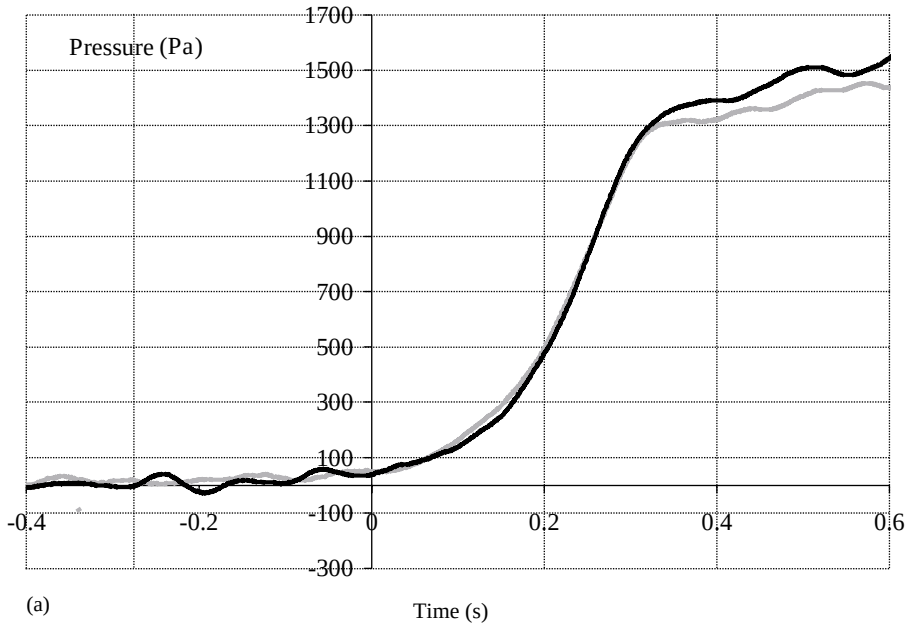

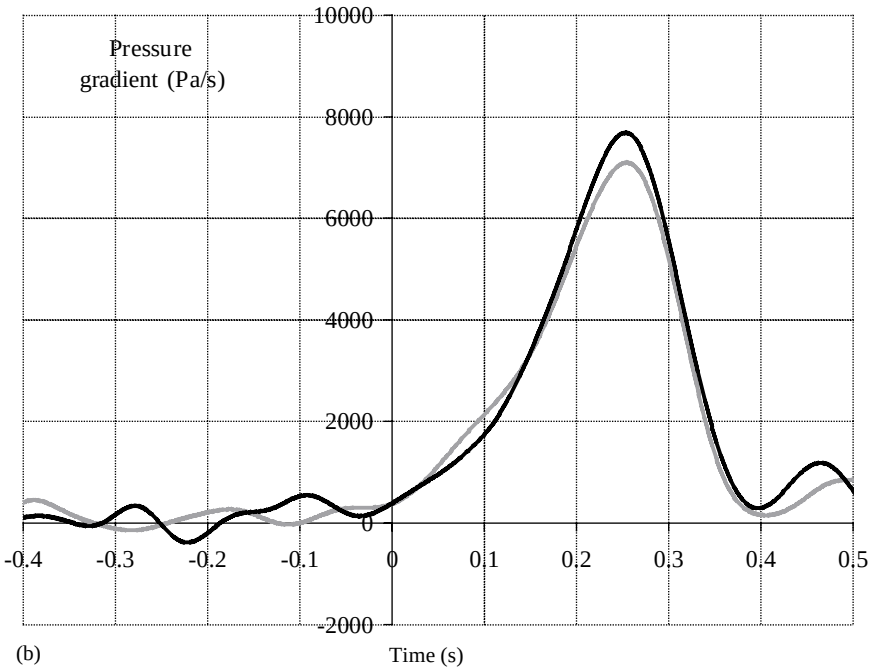

Fig. 10. Compression waves obtained with an axially symmetric nose (▬) and 3-D nose (—) at $X = 80$ m: (a) time evolution of the pressure; (b) time evolution of the pressure gradient.

formula proposed by Matsuo *et al*. also yields a good agreement, given the optimisation of a corrective coefficient corresponding to the train nose shape.

The possibility of replacing a three-dimensional train model by an equivalent axially symmetrical one has been evaluated to be valid, when the interest is limited to the planar

wave established at a distance measured from the tunnel entrance longer than about four times the tunnel diameter. We can then conclude that the optimal longitudinal cross-sectional area profile of the train nose in terms of the compression wave in the tunnel can be deduced using axially symmetrical models, while the drag and aerodynamic stability optimisation in open air should be realised by means of 3-D models with the above-determined sectional-area profile.

ACKNOWLEDGEMENTS

This work was partly supported by the European Union in the framework of a TRANSAERO research project. The authors gratefully acknowledge the co-contractors of the project, namely the three railway operators: DB AG, SNCF and FS who carried out difficult full-scale tests. Moreover, the authors want to thank Mr Destor, who prepared reduced-scale models.

REFERENCES

AOKI, T., MATSUO, K., HIDAKA, H., NOGUSHI, Y. & MORIHARA, S. 1995 Attenuation and distortion of propagating compression waves in a high-speed railway model and in real tunnels. Shock Waves in condensed matter and heterogeneous media. In: *Shock Waves Marseille* eds R. BRUN & L. Z. DUMITRESCU, pp. 347–352. Berlin:Springer-Verlag.

AUVITY, B. 1998 Phénomènes aérodynamiques instationnaires générées par l'entrée d'un train dans un tunnel. Ph.D. Thesis, University of Poitiers, France.

AUVITY, B., BELLENOUE, M. & KAGEYAMA, T. 2001 Experimental study of the unsteady aerodynamic field outside a tunnel during a train entry. *Experiments in Fluids* **30,** 221–228.

AUVITY, B. & KAGEYAMA, T. 1996 Etude expérimentale et numérique de l'onde de compression générée par l'entrée d'un train dans un tunnel. *Comptes Rendus de l'Académie des Sciences*, Paris, t. 323, Série IIb, Mécanique des Fluides, pp. 87–94.

BELLENOUE, M., AUVITY, B., MORINIERE, V. & KAGEYAMA, T. 1999 Etude des principaux paramètres influencant l'onde de compression générées par l'entrée d'un train dans un tunnel. *14ème Congrès Francais de Mécanique*, Toulouse, France, ISBN 2-84088-040-7 221–228.

DEMMENIE, E.A., DE BRUIN, A. C. & KLAVER, E. 1998 Experimental pressure wave research at NLR for high-speed rail tunnels. Report of the National Aerospace Laboratory NLR, No. NLR-TR-98375.

FOX, J. A. & VARDY, A. E. 1973 The generation and alleviation of air pressure transients in tunnels. *Tunnels and Tunnelling* Nov., 575–585.

GRÉGOIRE, R., RETY, J. M., MASBERBAT, F., MORINIÈRE, V., BELLENOUE, M. & KAGEYAMA, T. 1997 Experimental study (scale 1/70th) and numerical simulation of the generation of pressure waves and micro-pressure waves due to high-speed train–tunnel entry. *9th Aerodynamics and Ventilation of Vehicle Tunnels*, BHR Group Conference Series Publication No. 27, pp. 877–903, ISBN 1 86058 092 0.

HOWE, M. S. 1998*a* Mach number dependence of the compression wave generated by a high-speed train entering a tunnel. *Journal of Sound and Vibration* **212**, 23–36.

HOWE, M.S. 1998*b* Prolongation of the rise time of the compression wave generated when a high-speed train entering a tunnel. *Proceedings of the Royal Society (London)* A **455,** 863–878.

HOWE, M. S. 1998*c* The compression wave produced by high-speed train entering a tunnel. *Proceedings of the Royal Society (London)* A **454,** 1523–1534.

HOWE, M. S. 1999 On the compression wave generated when a high-speed train enters a tunnel with a flared portal. *Journal of Fluids and Structures* 13, 481–498.

IIDA, M. 1994 Numerical simulation of compression wave in tunnels during train nose entry. R.T.R.I. Report, Vol. 8, No. 6, pp. 25–30 (in Japanese).

IIDA, M., MATSUMURA, T., NAKATANI, K., FUKUDA, T. & MAEDA, T. 1996 Optimum nose shape for reducing tunnel sonic boom. *Institution of Mechanical Engineers (London)* Paper C514/015/96.

JOHNSON, T. 1999 1/25 Scale moving model tests for the TRANSAERO project. *TRANSAERO Symposium* (Transient Aerodynamics Railway System Optimisation), Paris, France.

KAGE, K., KAWAGOE, S. & MATSUO, K. 1992 Numerical study of compression waves by high speed trains entering a tunnel. Transactions of JSME Series B, 58, No. 547, pp. 815–819 (in Japanese).

KOHAMA, Y., HORIE, M. & YUKAWA, H. 1994 Shape of the high speed train head with high overall performances. *Nagar*e No. 13, Japan Fluid-Dynamics Association (in Japanese).

MAEDA, T., MATSUMURA, T., IIDA, M., NAKATANI, K. & UCHIDA, K. 1993 Effect of shape of train nose on compression wave generated by train entering tunnel. *International Conference on Speedup Technology for Railway and Maglev Vehicles*, Yokohama, Japan, pp. 315–319.

MATSCHKE, G. 1999 Full scale tests on pressure wave effects in tunnel. TRANSAERO Symposium (Transient Aerodynamics Railway System Optimisation), Paris, France.

MATSUO, K., AOKI, T., MASHIMO, S. & NAKASTU, E. 1997 Entry Compression wave generated by a high-speed train entering a tunnel. *Proceedings of the 9th Aerodynamics and Ventilation of Vehicle Tunnels*. BHR Group Conference Series Publication No. 27, pp. 925–934, ISBN 1 86058 092 0.

OGAWA, T. & FUJII, K. 1996 Prediction of wavefront of compression wave generated by a train moving into a tunnel with steady flow. *Transactions of JSME* Series B, Vol. 61, No. 586, pp. 2136–2142 (in Japanese).

OZAWA, S. & MAEDA, T. 1988 Tunnel entrance hoods for reduction of micro-pressue wave. *Quarterly of R.T.R.I.* **29,** 134–139.

OZAWA, S., MAEDA, T., MATSUMURA, T., UCHIDA, K., KAJIYAMA, H. & TANEMOTO, K. 1991 Countermeasures to reduce micro-pressure waves radiating from exits of Shinkansen tunnels. *Proceedings of the 7th International Symposium on Aerodynamics and Ventilation of Vehicle Tunnels*, Brighton, U.K., pp. 253–266. Amsterdam: Elsevier Science Publishers.

OZAWA, S. 1979 Study of micro-pressure wave radiated from a tunnel exit. Railway Technical Research Report (in Japanese).

OZAWA, S., MAEDA, T., MATSUMURA, T. & UCHIDA, K. 1993 Micro-pressure waves radiating from exits of Shinkansen tunnels. *Quartely reports of R.T.R.I.* **34,** 134–140.

SASOH, A., ONODERA, O., TAKAYAMA, K., KANEKO, R. & MATSUI, Y. 1994 Experimental study of shock wave generated by high speed train entry into a tunnel. *Transaction of JSME Paper* Series B, Vol. 60, No. 575, pp. 71–78.

SWARDEN, M. C. 1973 Vehicle-tunnel entry at subsonic speeds. Final Report — Part II, Report No. FRA-RT-73-16 / DSR 76111-4, Prepared for United States Department of Transportation.

WOODS, W. A., & POPE, C. W. 1979 On the range of validity of simplified one-dimensionnal theories for calculating unsteady flows in raiway tunnels. Proceedings of the *3rd International Symposim on Aerodynamics and Ventilation of Vehicle Tunnels*, Sheffield, U.K.

WOODS, W. A. & POPE, C. W. 1981 A generalised flow prediction method for the unsteady flow generated by a train in a single-track tunnel. *Journal of Wind Engineering and Industrial Aerodynamics* **7,** 331–360.